

4 VIBRATIONAL RELAXATION IN HDO:D₂O

We present a study on the relaxation of the OH stretch vibration in a dilute HDO:D₂O solution using femtosecond mid-infrared pump-probe spectroscopy. We performed one-color experiments in which the $0 \rightarrow 1$ vibrational transition is probed at different frequencies and two-color experiments in which the $1 \rightarrow 2$ transition is probed. In the one-color experiments, it is observed that the relaxation is faster at the blue side than at the center of the absorption band. Furthermore it is observed that the vibrational relaxation time T_1 shows an anomalous temperature dependence and increases from 0.74(1) ps at 298 K to 0.90(2) ps at 363 K. These results indicate that the OH \cdots O hydrogen bond forms the dominant accepting mode in the vibrational relaxation of the OH stretch vibration.

4.1 INTRODUCTION

In any pump-probe experiment (§1.2) on the OH stretch vibration of an aqueous system, the most prominent feature is vibrational relaxation: vibrationally excited OH bonds stay excited during a few picoseconds at most. Because vibrational relaxation means that energy is transferred to other degrees of freedom, a measurement of the vibrational lifetime T_1 provides information on inelastic interactions. The temperature dependence of T_1 can help to identify the modes to which the energy of the excited OH stretch vibration is transferred.⁹⁰ Typically, the lifetime decreases with increasing temperature.

A wide range of vibrational lifetimes has been reported for the OH stretch vibration of HDO dissolved in D₂O. The first experiments on its vibrational relaxation reported $T_1 = 8(2)$ ps (based on time-resolved experiments with 11 ps pulses⁴⁵) and $T_1 = 0.45(15)$ ps (based on saturation with high-intensity light¹²⁴). More recently, experiments with shorter pulses (0.2–0.5 ps) yielded values ranging from 0.7 to 1.0 ps.^{33,67,132}

This chapter presents a detailed investigation of the relaxation mechanism of the OH stretch vibration of HDO dissolved in D₂O. We measured the relaxation rate as a function of temperature for both the $0 \rightarrow 1$ and the $1 \rightarrow 2$ vibrational transitions. The combination of these experiments enables us to identify the vibrational relaxation mechanism.

4.2 EXPERIMENT

The experiments were pump-probe measurements where a femtosecond infrared laser pulse excited the $\nu = 0 \rightarrow 1$ transition of the OH stretch vibration of HDO molecules dissolved in D₂O. The transmittance of a subsequent probe pulse is a measure of the degree of excitation of the OH groups in the solution. The probe pulse was either at the same frequency (one-color experiments) or at a different frequency (two-color experiments). The general background on pump-probe experiments is discussed in §1.2; the details of the pulse generation in §2.2.3 and §2.2.4; and the pump-probe setup in §2.4.2. The sample was a 500 μm -thick layer of a HDO:D₂O solution in a sample cell that was continuously

rotated to eliminate local accumulation of heat (§2.8) and that was equipped with a heater that enabled us to control the temperature within 1 K. For the data in Fig. 4.2 we employed a cryostatic cell that was not rotated. To prevent local heating in this cell, we lowered the repetition rate of the laser from 1 kHz to 70 Hz. By use of polarizers (in the one-color experiments) or a magic-angle polarization (in the two-color experiments), we ensured that the measured signals are not sensitive to the reorientational motions of the individual HDO molecules.

4.3 RESULTS

In order to investigate the lifetime of the OH stretch vibration, we first carried out two-color experiments in which the $0 \rightarrow 1$ transition is pumped and the $1 \rightarrow 2$ transition is probed. Figure 4.1 shows typical measurements at different temperatures. In this experiment, the time constant of the decay is equal to the vibrational relaxation time, since the absorbance change is directly proportional to the excited population in the $\nu = 1$ state. The relaxation time T_1 is thus obtained by fitting the data to a single-exponential decay.

For small delay times the measured signals can be influenced by effects other than the vibrational relaxation. (i) The signals are strongly affected by spectral diffusion: due to the inhomogeneous broadening of the absorption band, the pump pulse excites only a part of the absorption band, which leads to the formation of a spectral hole. In liquid water the spectral diffusion takes place on a sub-picosecond timescale^{33,134} and is virtually complete after 1 ps. In Chapter 8, we will discuss this spectral diffusion in more detail. (ii) Not unlikely, the vibrational relaxation rate varies over the absorption band, which can affect the measured signals at small delay times. However, when the spectral relaxation is complete, one will observe only one effective average decay time, independent of the probing frequency. (iii) We cannot completely exclude the artifacts mentioned in §2.6 under point 6 and 7 (the former for the one-color experiments discussed later).

Because of these effects at short delay times, we fitted our data on liquid water only for delay values larger than 1.0 ps. Since the relaxation in ice turns out to be much faster, we fitted the data obtained for ice for delays larger than 0.4 ps.

Figure 4.2 shows the vibrational relaxation times measured in the two-color experiments for both frozen and liquid HDO:D₂O.¹³⁴ It shows that in the solid phase (ice-*Ih*), the relaxation time is virtually independent of temperature with an average value of 0.37(2) ps, and in liquid water the relaxation time increases with temperature from 0.74(1 ps at 270 K to 0.90(2) ps at 363 K.

Figure 4.3 shows typical measurements for a one- and a two-color experiment, at a temperature of 363 K. The decay times are 1.05(2) and 0.90(2) ps, respectively. Clearly, the one-color data show a slower decay than the two-color data.

Figure 4.4 shows an overview of the decay times for different frequencies and temperatures above the melting point of D₂O (277 K). It shows that for all temperatures, the decay of the absorbance change $\Delta\alpha$ is slower in the one-color measurements as compared to the data of the two-color experiments. Moreover, in the one-color experiments, the decay time constant increases as the frequency is shifted from the blue side (3500 cm⁻¹) to the center (3400 cm⁻¹) of the absorption band.

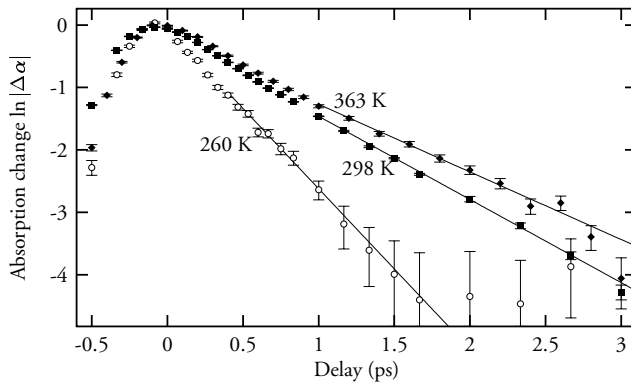


FIGURE 4.1. Typical normalized magic angle two-color measurements on solid (260 K) and liquid (298 and 363 K) HDO in D₂O at different temperatures. In liquid water, the pump and probe frequencies were 3400 and 3150 cm⁻¹, respectively. In ice, the frequencies were 3330 and 3090 cm⁻¹, respectively.

4.4 INTERMEDIATE-STATE MODEL

The results from the one-color experiments at 3400 cm⁻¹ and 3500 cm⁻¹, shown in Fig. 4.4, suggest a frequency dependence of the vibrational relaxation time. However, due to the fast spectral relaxation, discussed in Section 4.3,^{33,134} this cannot cause a different decay rate of the observed signal for delays larger than 1 ps.

We can explain the one-color data having a slower decay than the two-color data if the excited HDO molecule does not relax directly to the ground state, but rather to an intermediate state. This can be shown as follows. The absorbance change for a transition $a \rightarrow b$ is

$$\Delta \alpha_{a \rightarrow b} = \rho \sigma_{ab} (\Delta n_a - \Delta n_b), \quad (4.1)$$

where ρ is the number of molecules per unit area, σ_{ab} is the cross-section for a radiative transition and Δn_a and Δn_b are the changes in populations of the two levels with respect to the equilibrium populations. In a two-color experiment, the decay of the absorbance change $\Delta \alpha_{1 \rightarrow 2}$ induced by the pump only depends on the decay of Δn_1 , since the $v = 2$ state is not populated. However, in a one-color experiment, the absorbance change $\Delta \alpha_{0 \rightarrow 1}$ depends on both Δn_1 and Δn_0 . If, due to an intermediate state, the decays of Δn_0 and Δn_1 are not equal, this will influence the relaxation of the observed absorbance change.

In the following quantitative description, we label the intermediate state as $|o^*\rangle$. This intermediate state $|o^*\rangle$ is a combination of the ground state of the OH stretch mode and other modes that were excited by the energy release from the $v = 1$ state decay. Consequently, the $|o^*\rangle$ state can be excited to a $|1^*\rangle$ state, where both the OH stretch mode and the unknown other modes are excited. Due to anharmonic coupling, the center frequency of this $o^* \rightarrow 1^*$ transition can differ from the ordinary $o \rightarrow 1$ transition. Hence, the cross sections at a given laser frequency can differ. With cross sections σ^* for the $o^* \rightarrow 1^*$ and σ for the $o \rightarrow 1$ transitions, we can extend Eq. (4.1) to

$$-\Delta \alpha_{o1}(t) = \rho \sigma [\Delta n_o(t) - \Delta n_1(t) + (\sigma^*/\sigma) \Delta n_{o^*}(t)] \quad (4.2)$$

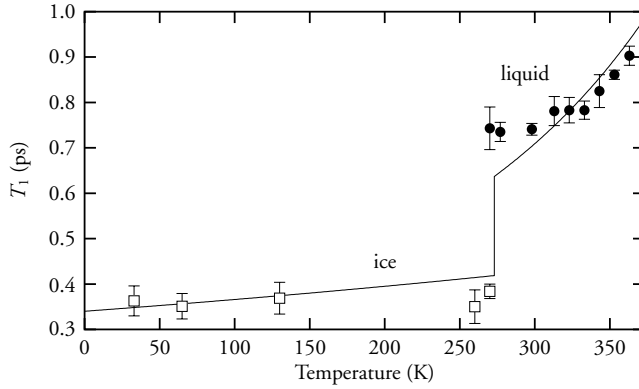


FIGURE 4.2. Vibrational relaxation time of the OH-stretch vibration of HDO in D₂O, measured in two-color measurements. The open and closed symbols denote results in ice and liquid water, respectively. The drawn line corresponds to Eq. (4.7).

Clearly, the measured decay depends on the value of the cross-section ratio σ^*/σ at the probing frequency.

If the rate for the $1 \rightarrow o^*$ relaxation process is given by k_A , and for the $o^* \rightarrow o$ relaxation by k_B (See Fig. 4.5), the dynamics of the population changes of the states satisfy the differential equation

$$\frac{d}{dt} \begin{pmatrix} \Delta n_1(t) \\ \Delta n_{o^*}(t) \\ \Delta n_o(t) \end{pmatrix} = \begin{pmatrix} -k_A & 0 & 0 \\ k_A & -k_B & 0 \\ 0 & k_B & 0 \end{pmatrix} \begin{pmatrix} \Delta n_1(t) \\ \Delta n_{o^*}(t) \\ \Delta n_o(t) \end{pmatrix}. \quad (4.3)$$

Its solution, expressed in the population changes at $t = 0$, is

$$\begin{pmatrix} \Delta n_1(t) \\ \Delta n_{o^*}(t) \\ \Delta n_o(t) \end{pmatrix} = M(t) \begin{pmatrix} \Delta n_1(0) \\ \Delta n_{o^*}(0) \\ \Delta n_o(0) \end{pmatrix}, \quad (4.4)$$

where

$$M(t) = \begin{pmatrix} e^{-k_A t} & 0 & 0 \\ \frac{k_A}{k_B - k_A} (e^{-k_A t} - e^{-k_B t}) & e^{-k_B t} & 0 \\ \frac{1}{k_A - k_B} (k_B e^{-k_A t} - k_A e^{-k_B t}) + 1 & 1 - e^{-k_B t} & 1 \end{pmatrix}. \quad (4.5)$$

We can combine Eqs. (4.2) and (4.4) with the initial values

$$(\Delta n_1(0), \Delta n_{o^*}(0), \Delta n_o(0)) = a(1, 0, -1) \quad (4.6)$$

defined by the pump pulse excitation, where a is an arbitrary amplitude. The parameters k_A , k_B , and σ^*/σ must be derived from the actual data. The value k_A follows directly from the two-color experiments in which the $1 \rightarrow 2$ transition is probed ($k_A = 1/T_1$ as in Fig. 4.2). Knowing k_A , we can use the one-color data to find the values for k_B and σ^*/σ . As

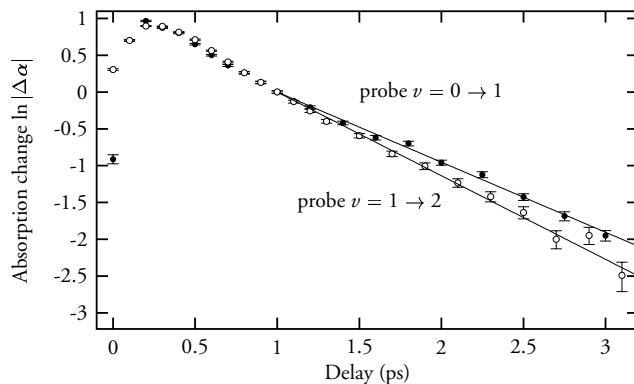


FIGURE 4.3. Typical delay scans for the isotropic absorbance change in dilute HDO:D₂O, after excitation at 3400 cm⁻¹. The temperature was 363 K and the data are normalized at $t = 1.0$ ps. The drawn lines are fits to exponentials. Note the difference in decay rates.

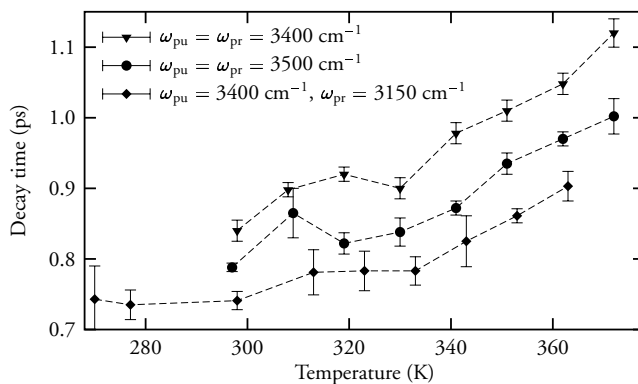
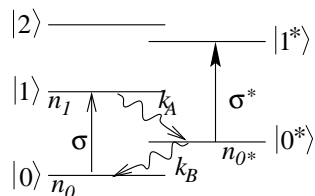


FIGURE 4.4. Vibrational decay time constant for different temperatures as found in one- and two-color experiments.

FIGURE 4.5. States and quantities used in the analysis. The states on the left are pure excitations of the OH vibration, while the states on the right are combinations of OH vibrational excitations and excitations of other modes.



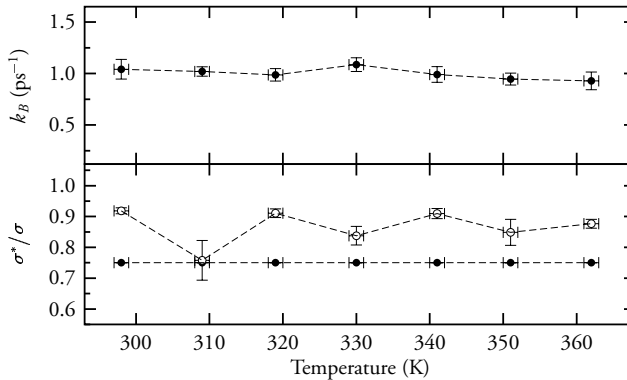


FIGURE 4.6. The decay rate k_B and the cross-section ratio σ^*/σ as a function of temperature. In the upper half, the decay rate k_B is shown that results from fitting the data at 3400 cm^{-1} , with the cross-section ratio σ^*/σ fixed at 0.75. These k_B values are used to find the cross sections at 3500 cm^{-1} in the bottom half (open symbols). For comparison, the fixed cross-section at 3400 cm^{-1} is shown as well (closed symbols).

the difference between the one-color and two-color data is most prominent at the center of the absorption band (3400 cm^{-1}), a first attempt is to fit values for k_B and σ^*/σ at that frequency. Since the two-color data were obtained at slightly different temperatures, we interpolated the k_A values linearly from the nearest temperatures above and below. However, because the quantities k_B and σ^*/σ are mathematically strongly correlated, it is difficult to determine them independently from each other within the accuracy of the experimental data.

It is reasonable to assume that the cross-section ratio σ^*/σ does not depend strongly on temperature. The vibrational relaxation of the OH vibration leads to a transfer of approximately 3400 cm^{-1} to a few accepting modes. If there would be only one accepting mode, the resulting degree of excitation of this mode would correspond to a thermal distribution at a temperature of approximately 5000 K. We can therefore expect that the comparatively small range of temperatures in our measurements does not have much influence on the cross-section ratio σ^*/σ of the intermediate state and we assume that σ^*/σ has a constant value. The values for σ^*/σ obtained from the first fit varied between 0.55 and 0.95 ps; we therefore assume that $\sigma^*/\sigma = 0.75(20)$ and use this value as a fixed parameter to fit all data with pump and probe frequency at 3400 cm^{-1} . This procedure yields values for k_B as a function of temperature, as shown in the upper half of Fig. 4.4. With this approach, there is clearly no significant temperature dependence. Using these k_B values, we can now fit the cross-sections at the 3500 cm^{-1} probe frequency, as shown in Fig. 4.4. At 3500 cm^{-1} , the cross section σ^* is systematically larger compared to 3400 cm^{-1} , with no significant temperature dependence. The latter confirms that both k_B and σ^*/σ are not significantly dependent. However, the uncertainty in σ^*/σ of approximately ± 0.2 causes an error in the value of k_B . By repeating the procedure for the 3400 cm^{-1} data with $\sigma^*/\sigma = 0.55$ and 0.95, we find that $k_B = 1.0(5)\text{ ps}^{-1}$. In all three cases, we find that the cross-section σ^* at 3500 cm^{-1} is systematically larger than the cross-section at 3400 cm^{-1} .

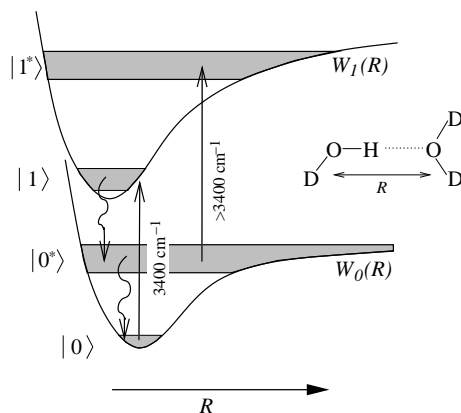


FIGURE 4.7. Schematic potentials $W_v(R)$ of the hydrogen bond mode, for the $\nu = 0$ and $\nu = 1$ OH stretch states. Shown are the proposed $|0\rangle$, $|1\rangle$, $|0^*\rangle$, and $|1^*\rangle$ states, the central excitation frequencies and the non-radiative decay paths.

4.5 DISCUSSION

The systematically larger cross-sections at 3500 cm^{-1} compared to 3400 cm^{-1} suggest that the $0^* \rightarrow 1^*$ transition has a blue-shifted frequency with respect to the normal OH stretch excitation. This is quite surprising, since excitation of other anharmonically coupled molecular modes leads normally to a redshift of the vibrational frequency^{43,42}. However, the blueshift can be well explained if the $|0^*\rangle$ state is an OH-stretch $\nu = 0$ state in combination with a highly excited hydrogen-bond stretch state. The $|1^*\rangle$ state then corresponds to the case where both the hydrogen bond and the OH bond are excited. A qualitative picture of the energy levels involved is shown in Fig. 4.7. Figure 8.3 on page 91 shows a more quantitative calculation of these potentials.

In principle, the hydrogen-bond dynamics within each of the hydrogen-bond potentials $W_v(R)$ could be calculated by solving the one-dimensional Schrödinger equation in R with $W_v(R)$ as the potential. This type of description would be appropriate for gas-phase hydrogen-bonded clusters in which the hydrogen-bond vibration is nearly undamped. For these systems, the coupling between the OH stretch vibration and the hydrogen-bond mode leads to a hydrogen-bond vibrational (Franck-Condon) progression of the absorption spectrum of the OH stretch vibration.¹⁰¹ However, in the liquid phase, the transient (Chapter 8) and linear absorption spectra of HDO:D₂O (Fig. 1.3 on page 13) do not contain sidebands and are very broad. This indicates that the hydrogen-bond vibrations of liquid water are strongly overdamped, which implies that the wavefunctions in R are strongly coupled to each other and to other low-frequency liquid modes. The dynamics in R are therefore not determined by the level spacing of the unperturbed vibrational levels of the hydrogen-bond mode, but result rather from a stochastic modulation of the value of R due to the interactions with the surrounding liquid. This type of dynamics can best be described as a diffusion process in the potential $W_v(R)$, as we will see in Chapter 5.

We must note here that it is a conceptual simplification to regard $|0^*\rangle$ as a single and well-defined state. A more accurate description would involve a broad band of hydrogen bond energy levels, each of which causes a different blueshift and cross-section of the OH stretch transition. In principle, application of such a model would give more detailed information on the lifetime of each individual excited quantum state of the hydrogen bond. However, the fact that the data can be described satisfactorily with a single intermediate

state $|0^*\rangle$) and a single relaxation rate constant $k_B = 1.0(5) \text{ ps}^{-1}$ shows that our experimental limitations do not allow us to obtain information about these more subtle details. Therefore we limit ourselves to a lifetime for the average excitation level of the hydrogen bond.

Apart from the relaxation through the hydrogen bond, there may be other relaxation channels, in which either all OH stretch energy is transferred to a low-frequency mode other than the hydrogen-bond stretch, or in which the OH stretch energy is distributed over several modes, amongst which the hydrogen-bond mode. In the latter case, the hydrogen-bond mode does not receive the entire 3400 cm^{-1} of the OH stretch energy, but only some fraction. However, other accepting modes such as the intramolecular bend mode are likely to cause a small transient redshift,^{42,43} as opposed to the present blueshift, while modes in neighboring D₂O molecules would not cause any significant frequency shift at all. Therefore, the hydrogen-bond stretch mode must account for a significant fraction of the OH-stretch decay. Other candidates for accepting modes include the OD stretch of HDO (further denoted as ν_{1a}) at 2500 cm^{-1} , the OD stretch of D₂O (ν_{1b} , 2500 cm^{-1}), the HOD bend (δ_1 , 1450 cm^{-1}), and the DOD bend (δ_2 , 1210 cm^{-1}). Recently, Deák et al.²¹ showed in a time-resolved anti-Stokes Raman study that relaxation following the excitation of the OH stretch in HDO:D₂O results in a population of ν_1 (1a and 1b are spectrally indistinguishable), of δ_1 , and of δ_2 . Upon decay of the OH stretch vibration, approximately 3400 cm^{-1} of energy must be transferred to its environment, the first step of which is normally the excitation of several other modes, that can be the hydrogen-bond stretch (which we have proposed in this chapter) or the mentioned ν and δ modes. In principle, several different relaxation pathways may occur with different probabilities. Deák et al.²¹ estimated that de-excitation of one OH stretch mode results in ≥ 0.6 quanta of δ_1 , ≥ 0.6 of δ_2 , and 0.1 of ν_1 . These estimates indicate that, on the average, still up to 1550 cm^{-1} of the energy of the OH stretch mode is donated to the hydrogen-bond stretch mode.

With the hydrogen bond as the dominant accepting mode, the anomalous temperature dependence of the vibrational relaxation time T_1 can also be explained. A theoretical model of the energy transfer from the OH stretch vibration to the OH...O hydrogen bond was developed by Staib and Hynes.¹¹⁴ Their model system consists of a single OH bond coupled to a single hydrogen bond. The coupling is described by Lippincott-Schroeder potentials, that incorporate the gas-phase OH-bond potential, the hydrogen bond, and the Van der Waals and electrostatic interactions. (these potentials will be discussed in detail in Chapter 8.) The hydrogen bond causes the OH stretch frequency to shift from the gas-phase frequency ω_{gas} to a condensed-phase frequency ω . The model shows that the vibrational lifetime $T_1(\text{OH})$ depends on this redshift as

$$T_1(\text{OH}) \propto (1 - \omega/\omega_{\text{gas}})^{-1.8}. \quad (4.7)$$

This relation has been verified experimentally for a wide range of hydrogen-bonded complexes⁸⁶ and can be understood qualitatively in the following way. The redshift of the absorption band of the OH stretch vibration induced by the hydrogen bond is a measure for the strength of the interaction between the hydrogen bond and the OH stretch vibration. If the interaction gets stronger, the rate of energy transfer to the hydrogen bond will be faster, leading to a shorter T_1 . When the temperature is increased, the absorption spectrum of the OH stretch vibration shifts towards higher frequencies, which implies that

the average hydrogen-bond strength in water decreases. This explains the increase of T_1 with temperature. By combining Eq. (4.7) with the known temperature dependence of the OH absorption band redshift²⁸, we can describe the T_1 data quite well (see Fig. 4.2).

The relaxation mechanism observed for HDO is to some extent analogous to the relaxation of the OH stretch vibration of ethanol clusters dissolved in carbon tetrachloride (CCl₄).^{46,66,133} In this system, the hydrogen bond is the main accepting mode in the relaxation of the OH stretch vibration. The energy that is transferred from the OH stretch vibration to the hydrogen bond causes the hydrogen bond to dissociate with a transient blue-shifted absorption of dissociated ethanol cluster fragments as a result. The hydrogen bond reassociation in the ethanol clusters is relatively slow and has a time constant of approximately 20 ps. For water, as we have seen, the relaxation of the hydrogen bond is much faster and has a time constant $1/k_B \approx 1$ ps. A likely reason for the fast hydrogen-bond relaxation in water is that, due to the network of hydrogen bonds, the energy can be dispersed very fast over the environment of the initially excited molecule. In contrast, in the experiment on ethanol dissolved in CCl₄, the CCl₄ environment does not provide efficient accepting modes and thus the hydrogen bond relaxes much slower.

4.6 CONCLUSIONS

Using femtosecond mid-infrared pump-probe experiments, we have measured the lifetime of the OH stretch vibration in liquid HDO in D₂O. For ice-*Ih*, the lifetime has a constant value of 0.37(2) ps over the range 33–270 K, while for liquid water, the lifetime increases from 0.74(2) ps at 270 K to 0.90(2) ps at 363 K. This temperature dependence is quite anomalous since in general it is observed that the vibrational lifetime decreases with temperature. If the 0 → 1 transition is probed, it is observed that the relaxation of the bleaching is faster at the blue side of the absorption band than at the center of the absorption band. Both this observation and the anomalous temperature dependence of the vibrational lifetime can be well explained if the OH ··· O hydrogen bond forms the main accepting mode in the vibrational relaxation of the OH stretch vibration. From a detailed analysis of the data we find that the excited hydrogen bond relaxes with a time constant of 1.0(5) ps. This relaxation is relatively fast compared to other hydrogen-bonded systems, which can be explained from the fact that the network of hydrogen bonds in liquid water allows a very rapid dissipation of energy.